PHYSICAL LAYER DESIGN FOR A BROADBAND OVERLAY SYSTEM IN THE VHF BAND

I. Cosovic, S. Brandes, M. Schnell, German Aerospace Center, DLR Oberpfaffenhofen, Wessling, Germany

B. Haindl, Frequentis GmbH, Vienna, Austria

Abstract

In this paper, the physical layer design of the B-VHF system is described and discussed. B-VHF is a broadband communications system for air-traffic control based on multi-carrier technology which is intended to be applied as an overlay system to the existing aeronautical communications systems in the VHF band. Special focus in this paper is put on the physical layer design challenges which have to be solved in order to guarantee the co-existence between B-VHF and the legacy VHF systems. Especially, the interference avoidance techniques at the B-VHF transmitter as well as the required interference suppression techniques at the B-VHF receiver are discussed in detail.

I. Introduction

In January 2004, the research project "Broadband VHF Aeronautical Communications System Based on Multi-Carrier Technology" (B-VHF) [1] started which is funded by the European Commission. The prime goal of this project is to verify the feasibility of a Multi-Carrier (MC) based overlay system for future Air Traffic Control (ATC) communications in the Very High Frequency (VHF) band which will operate simultaneously with the legacy VHF systems – Double Side-Band Amplitude Modulation (DSB-AM) and VHF Digital Link (VDL) – without degrading their performance. Within the project, measurement flights and worst-case simulations have been carried out to assess the available VHF spectrum for the B-VHF overlay system. The results indicate that significant amounts of VHF spectrum can be re-used by the B-VHF system. Thus, B-VHF allows a gradual in-band transition from the current to a future ATC communications system using an overlay concept.

This paper focuses on the physical layer design of the B-VHF system. Especially, the key design challenges related to the physical layer of an overlay system are addressed and solutions are proposed. The overlay concept is enabled by using MC technology based on Orthogonal Frequency-Division Multiplexing (OFDM). As OFDM based MC systems are very flexible and adjustable to certain spectrum restrictions, an adaptation to the available frequency gaps can easily be made. The main two design challenges of an OFDM based overlay system are the following. Suppression of the OFDM sidelobes at the B-VHF transmitter in order not to interfere with the legacy VHF systems and suppression of the legacy VHF system signals at the B-VHF receiver in order to guarantee acceptable B-VHF system performance. Besides others, these both design challenges will be discussed in detail in this paper.

The paper is organized as follows. The B-VHF system model is described in Section II. In Section III, the key physical layer design challenges of the B-VHF system are recognized. Especially, the avoidance of interference from B-VHF to the VHF legacy systems and the suppression of interference from VHF legacy systems at the B-VHF receiver are considered in detail. The performance of the B-VHF overlay system is presented in Section IV taking into account techniques that avoid interference from B-VHF to the VHF legacy systems. Finally, Section V concludes this paper.

II. System Model

The B-VHF system applies MC technology based on OFDM to enable the overlay concept. The principles of OFDM are well-known and not described here. For additional information see, e.g. [2, 3]. For the forward link – ground station to aircraft – OFDM is combined with Code-Division Multiple-Access (CDMA) resulting in MC-CDMA. Especially, the very flexible concept of MC-CDMA with M&Q modification [2, 3] is chosen which easily allows for an exchange between user capacity

0-7803-9307-4/05/$20.00 ©2005 IEEE.

and transmission data rate. Moreover, due to the CDMA component the B-VHF forward link is especially robust with respect to narrowband interference caused by the legacy VHF systems.

For the reverse link – aircraft to ground station – Orthogonal Frequency-Division Multiple-Access (OFDMA) is chosen, since this technique facilitates reverse link channel estimation considerably compared to MC-CDMA. For increasing the narrowband interference robustness an additional Code-Division Multiplexing (CDM) component and/or slow frequency-hopping is foreseen.

In Figure 1 the B-VHF overlay concept is shown schematically. For a more detailed description of the B-VHF overlay concept please refer to [2].

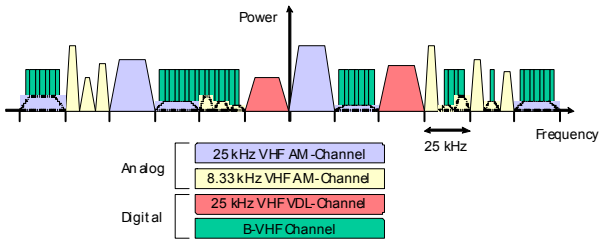

Figure 1. B-VHF Overlay Concept Showing the Co-Existence of DSB-AM and VDL Systems with the B-VHF System

III. Physical Layer Design Challenges

The fact that we deploy the B-VHF system using an overlay concept induces additional constraints on some parameters of the OFDM based MC system and even requires some additional parameters to describe the system. Most of the standard OFDM physical layer components do not need to be changed at all or only have to be slightly modified. A few components have to undergo more significant changes and even some new components have to be inserted. In order to fulfill the special requirements of an OFDM based overlay system the following issues have to be considered:

- Sub-carrier spacing;
- Flexible OFDM frame structure;
- Avoidance of interference from B-VHF to the VHF legacy systems;
- Suppression of interference from VHF legacy systems at the B-VHF receiver;
- Channel estimation;
- Synchronization.

Note that this list is not exhaustive, i.e., some further design challenges could be added.

Due to the space limitations of this paper, we concentrate on sub-carrier spacing, flexible OFDM frame structure, interference avoidance at the transmitter, and interference suppression at the receiver in the following and discuss these design challenges in detail.

Sub-Carrier Spacing

In OFDM systems sub-carrier spacing is usually chosen such that fading per sub-carrier can be considered as flat [3]. In addition to that, the B-VHF system design requires that the OFDM sub-carriers fit into the grid of 8.33 / 25 kHz DSB-AM channels, i.e., the sub-carrier spacing Δf has to be an integer multiple of the DSB-AM channel spacing. Furthermore, narrow sub-carrier spacing leads to a signal which is very sensitive to the influence of frequency offsets. The selection of sub-carrier spacing in the range of 1-4 kHz appears to be reasonable. For the B-VHF system sub-carrier spacing of $\Delta f = 2.083$ kHz is chosen, such that one 8.33 kHz DSB-AM channel spans 4 sub-carriers, and one 25 kHz channel 12 sub-carriers, respectively. With that sub-carrier spacing the expected Doppler induced inter-carrier interference (ICI) is still low while already having available a reasonable number of sub-carriers per DSB-AM channel. Figure 2 illustrates the sub-carrier spacing in the 8.33 kHz grid.

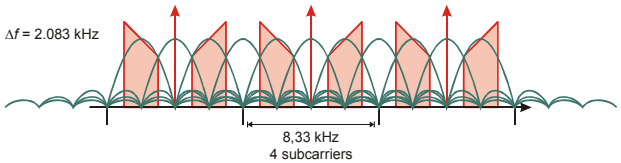

Figure 2. Sub-Carrier Spacing of $\Delta f = 2.083$ kHz Complying with the 8.33 kHz Grid

Flexible OFDM Frame Structure

In an OFDM based overlay system the standard OFDM frame structure cannot be used. It has to be adapted to the system's overlay structure.

The main difference is that in contrast to a standard OFDM system not the entire frequency band is available for transmission in an OFDM based overlay system. Narrowband VHF interference disables the exploitation of the complete frequency band for transmission of the OFDM signal.

Within the B-VHF project a classification between 'strong' and 'weak' VHF interferers is made. 'Strong' interferers are those whose emitted power, observed in a certain B-VHF cell, lies above a pre-defined limit. This pre-defined limit is carefully chosen in order to avoid interference from the B-VHF system to the legacy VHF systems. Note, the VHF channels occupied by the strong interferers are not used for B-VHF transmission, since the corresponding legacy VHF system receivers might be located close to the B-VHF transmitter. The emitted power of 'weak' VHF interferers is below the pre-defined limit which indicates that the corresponding VHF channels are either not used by any legacy VHF system or that the legacy VHF systems are sufficiently far away from the B-VHF cell and, thus, do not suffer from the B-VHF transmissions. Consequently, only the VHF channels with 'weak' interferers are used for transmission within a B-VHF cell. As no continuous frequency band is available for the B-VHF overlay system and only parts of the VHF band can be exploited for the B-VHF transmission the OFDM frame structure has to be adjusted to such conditions.

Furthermore, the frame structure has to be adaptable to the different spectrum allocation in different B-VHF cells. Such flexibility is inherently available in OFDM as with OFDM certain frequency ranges can be left empty by simply turning off the respective sub-carriers.

An example of the B-VHF OFDM frame structure is shown in Figure 3 assuming that parts of the transmission spectrum are occupied by 'strong' interferers and that no B-VHF signal is transmitted in these parts of the spectrum. The available spectrum can be used for the transmission of data, pilot, signaling, and sidelobe suppression symbols.

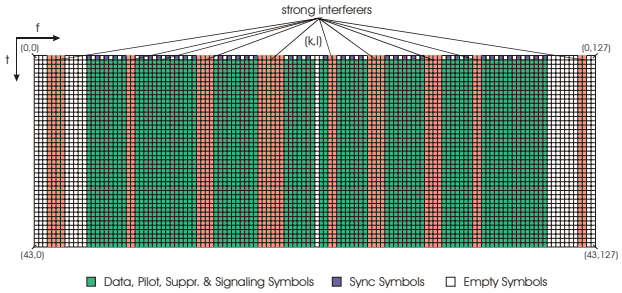

Figure 3. Flexible OFDM Frame Structure

Avoidance of Interference from B-VHF to the VHF Legacy Systems

Considering OFDM based overlay systems which utilize the frequency gaps of existing systems, out-of-band radiation has to be reduced in order to enable the co-existence of legacy systems and overlay system in the same frequency band. Hence, suppression of sidelobes is an important task in OFDM based overlay systems. In the following, three methods for sidelobe suppression are described.

Windowing

The sharp transitions between consecutive OFDM symbols and rapid amplitude changes increase the out-of-band radiation [4]. To reduce the out-of band radiation at the OFDM transmitter each OFDM symbol is multiplied with a windowing function in time domain. If the edges of the windowing function are less steep than the ones of the conventionally used rectangular window, the sharp phase transitions between OFDM symbols are smoothed. As a result of such windowing, each sub-carrier has lower sidelobes than with conventional rectangular windowing.

In this contribution, windowing is performed with the well-known Raised-Cosine (RC) pulse defined as

$$w(t)=\begin{cases}\frac{1}{2}+\frac{1}{2}\cos\left(\pi+\frac{\pi t}{\alpha T_o}\right), & 0\le t<\alpha T_o\\ 1, & \alpha T_o\le t<T_o\\ \frac{1}{2}+\frac{1}{2}\cos\left(\frac{\pi(t-T_o)}{\alpha T_o}\right), & T_o\le t<(1-\alpha)T_o\\ 0, & \text{else}\end{cases}, \quad (1)$$

where T_o is the useful length of an OFDM symbol. In addition, α is the so-called roll-off factor with

$0 \le \alpha \le 1$. If $\alpha = 0$, the RC pulse becomes a rectangular pulse and in this case out-of-band radiation is not reduced.

When windowing is applied the length of the considered OFDM segment has to be enlarged by a pre- and postfix as it is depicted in Figure 4. As the OFDM symbols partially overlap with adjacent OFDM symbols the length of pre- and postfix are chosen such that the OFDM symbol plus the Guard Interval (GI) lie in that region of the window which is not affected by the overlapping. The length of the prefix is chosen such that it spans the roll-off region and the GI, whereas the postfix only spans the roll-off region. Note, GI as well as pre- and postfix are cyclical extension of the OFDM symbol.

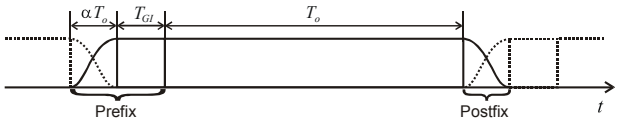

Figure 4. OFDM Signal in Time Domain

The drawback of windowing is that the system throughput is slightly reduced as OFDM symbols are prolonged in time domain. However, as shown in the following already for relatively low roll-off factors, e.g. $\alpha = 0.2$, a significant reduction of the out-of-band radiation is achieved.

To illustrate the effectiveness of windowing for sidelobe suppression we consider a Binary Phase-Shift Keying (BPSK) modulated OFDM system with $N = 12$ sub-carriers for data transmission. A number of 16 sidelobes from each side of the used spectrum is considered for the calculation of the sidelobe suppression. The roll-off factor of the RC pulse is kept variable.

The spectra of the OFDM signals of the original transmission sequence and of the transmission sequence after windowing are illustrated in Figure 5 for the symbol vector $\mathbf{d} = (1,1,1,1,1,1,1,1,1,1,1,1)^T$ assuming a roll-off factor $\alpha = 0.2$. The benefits of windowing are clearly visible. In comparison to OFDM with conventional rectangular windowing the sidelobes are suppressed by more than 10 dB.

In Figure 6 the mean Power Spectral Density (PSD) for all possible BPSK symbol vectors is shown for different roll-off factors. It can be noted that higher roll-off factors lead to better sidelobe suppression. However, higher roll-off factors lead to a further loss in throughput as symbols become longer in time domain [5].

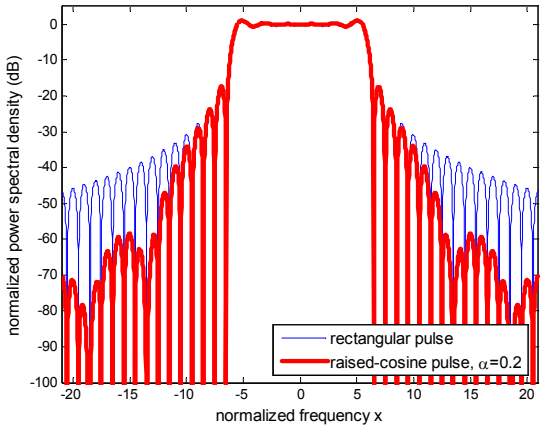

Figure 5. Spectrum of OFDM Signal with Rectangular and RC pulse ($\alpha = 0.2$); $\mathbf{d} = (1,1,1,1,1,1,1,1,1,1,1,1)^T$, $N = 12$

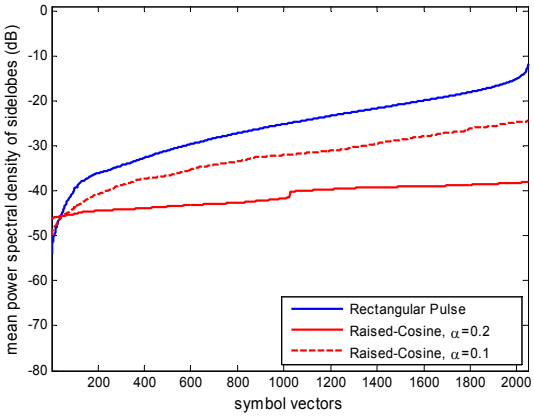

Figure 6. Mean Power Spectral Density of Sidelobes of All Possible BPSK Symbol Vectors with Different Pulse Shapes; $N = 12$

Insertion of Cancellation Carriers

In the following, an approach based on the insertion of a few so-called Cancellation Carriers (CC) on the left and right hand side of the used OFDM spectrum which suppress the sidelobes of the transmit signal is described [6, 7]. The CCs are not employed for data transmission, but carry complex weighting factors which are determined

such that the sidelobes of the CCs suppress the sidelobes of the original transmit signal. The basic principle of CCs is illustrated in Figure 7.

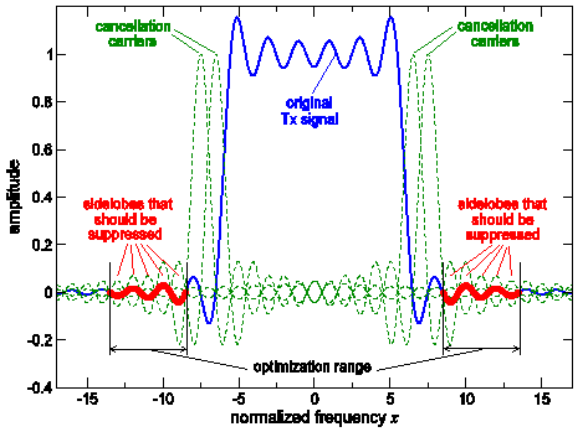

Figure 7. The Basic Principle of CCs

In [6] an approach in which CCs are determined as a linear combination of the corresponding data symbols is considered, whereas in [7] CCs are selected according to a least-squares optimization criterion. In this contribution the latter method is considered. For a complete description of this method including a detailed discussion of the optimization criterion, please refer to [7].

The sidelobe suppression achievable with CC is illustrated in Figure 8. For the symbol vector $\mathbf{d} = (1,1,1,1,1,1,1,1)^T$, the spectra of the OFDM signals without and with CCs are shown. Altogether 4 sub-carriers are used for sidelobe suppression – 2 on the left and 2 on the right side of the spectrum. The remaining 8 sub-carriers are used for data transmission. In the considered example, a suppression of sidelobes by more than 30 dB compared to the original OFDM signal is achieved. The drawback of sidelobe suppression by CC is that a certain amount of power has to be spent for the CCs and, thus, is not available for data transmission which leads to a slight degradation in Bit Error Rate (BER) performance.

In Figure 9 the mean PSD for all possible BPSK symbol vectors is shown for the case with and without CCs. With the application of CCs an average suppression of about 14 dB in comparison to the case without CCs is achieved. In this case, the power spent for the CCs is limited to 25% of the total transmission power. When a larger amount of transmission power is available for the CCs a better suppression is achieved, but at the same time the system performance further degrades.

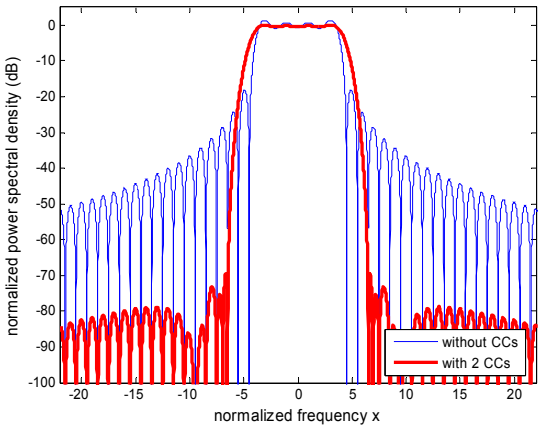

Figure 8. Spectrum of OFDM Signal Without and With 2 CCs at Each Side;
$\mathbf{d} = (1,1,1,1,1,1,1,1)^T$, $N = 12$, 4 CCs.

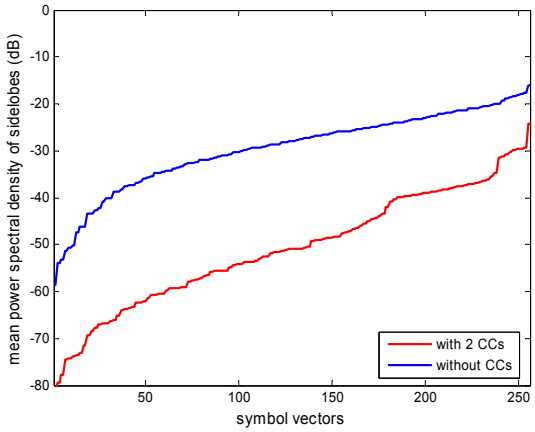

Figure 9. Mean PSD of Sidelobes of All Possible BPSK Symbol Vectors without and with CCs.

Carrier Weighting

A different approach for sidelobe suppression is Carrier Weighting (CW). In this approach, all sub-carriers are used for data transmission, but weighted by real-valued factors which are chosen in order to minimize the sidelobes. A detailed discussion of CW including optimization strategies can be found in [8].

The principle of the CW technique is illustrated in Figure 10 and Figure 11. From these figures it can be seen that in the case of CW the signals of the individual sub-carriers are adapted so as to mainly cancel each other in the optimization range. As a consequence, in the case of CW the sidelobes of the sum signal exhibit significantly lower values in the optimization range compared to the non-weighted sum signal. In order to guarantee that each sub-carrier receives a certain amount of transmission power, an upper limit $g_{\max}$ and a lower limit $g_{\min}$ on the weighting factors are introduced, respectively. The selection of weighting factors is performed by using an optimization algorithm as described in [8].

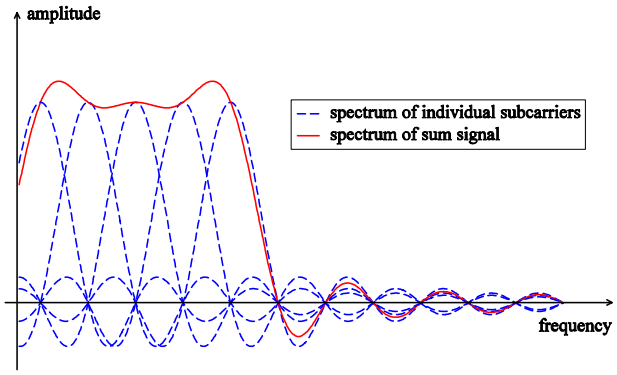

Figure 10. Spectrum of Standard OFDM Signal without CW

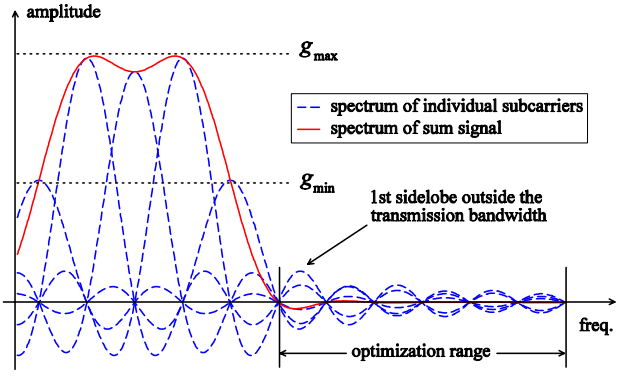

Figure 11. Spectrum of OFDM Signal with CW

The drawback of the CW method is a slight loss in BER performance as with weighting different sub-carriers have different amounts of power for transmission.

The spectra of the OFDM signals with and without CW are illustrated in Figure 12 for the symbol vector $\mathbf{d} = (1,1,1,1,1,1,1,1,1,1,1,1)^T$. In the case of CW the ratio of $\rho = g_{\max}/g_{\min} = \sqrt{4}$ is used. The benefits of the CW technique are clearly visible. In comparison to OFDM without CW the sidelobes are suppressed by more than 10 dB in the optimization range.

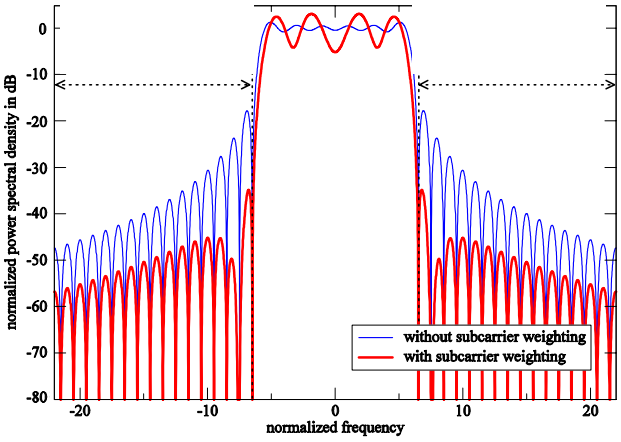

Figure 12. Spectrum of OFDM Signal with and without CW; $N = 12$, $\rho = \sqrt{4}$, $\mathbf{d} = (1,1,1,1,1,1,1,1,1,1,1,1)^T$

The sidelobe suppression averaged over all possible BPSK data symbol sequences for OFDM with $N = 12$ sub-carriers applying CW is summarized in Table 1. The simulation results are given for different ratios ρ. To calculate the average sidelobe suppression, standard OFDM without CW is taken as a reference. It is noticeable that already for $\rho = \sqrt{4}$ a remarkable average suppression of more than 10 dB is achieved. A further increase of the ratio ρ enables even better suppression. The reason for this lies in the fact that as this ratio grows the constraint becomes looser, thus allowing more degrees of freedom to find a solution of the optimization problem. However, enlarging the ratio ρ simultaneously leads to a further loss in BER performance as sub-carriers receive unequal amount of transmission power [8]. Therefore, there is a trade-off between the additional sidelobe suppression obtained by

enlarging the ratio ρ and the increased loss in BER performance.

Table 1. Average Sidelobe Suppression for OFDM applying CW for Different Ratios ρ

Ratio $\rho = g_{max} / g_{min}$	$\sqrt{2}$	$\sqrt{4}$	$\sqrt{6}$	$\sqrt{8}$
Average sidelobe suppression in dB	4.9	10.2	13.4	15.8

Suppression of Interference from VHF Legacy Systems at the B-VHF Receiver

The interference suppression and mitigation at the B-VHF receiver is necessary to reduce the power of the interference signals coming from the legacy VHF systems. The suppression of the interferer should take place as early as possible within the B-VHF receiver, in order to minimize performance requirements on the Analogue-to-Digital Converter (ADC) and the digital signal processing chain. In general, interference suppression modules can be implemented at the following position within the B-VHF receiver:

- Analogue domain: At the analogue front-end a Radio Frequency Interference (RFI) suppression module can reduce the power of all strong interferers in order to reduce the requirements on the ADC. This is especially of interest in the case where the own transmitted DSB-AM signal at an airplane is within the B-VHF bandwidth, since this signal causes very strong interference. However, this signal can easily be measured and effectively subtracted in the analogue front-end. Note, other suppression approaches at the analogue side, like adaptive notch filtering, are limited, since they are expensive and cause inter-symbol and inter-carrier interferences [9].
- Digital time domain: In time domain an adaptive digital RFI canceller and/or windowing can suppress strong and weak interferers. This approach is necessary to reduce the leakage effect which occurs if interference signals are transformed into frequency domain using the discrete Fourier transform [9].
- Digital frequency domain: In frequency domain the remaining leakage effect can be suppressed applying digital signal processing. Moreover, a soft erasure module and interference dependent equalizer can provide additional interference suppression [10].

Figure 13 shows a functional block diagram of a B-VHF receiver where all different interference cancellation modules are displayed. The functional blocks related to RFI cancellation are shaded. RFI cancelling is performed in multiple stages: Pre-suppression at the analogue front-end, windowing in the digital time domain, and suppression of the residual RFI in frequency domain. In the following the different methods will be described in detail.

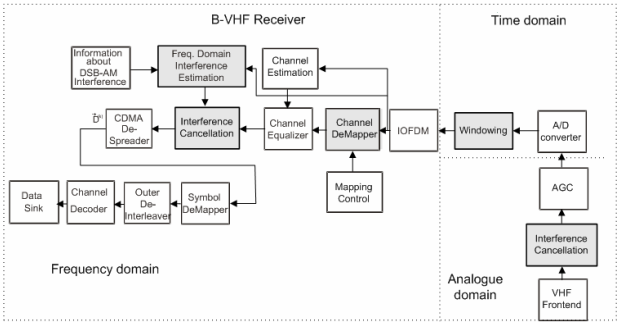

Figure 13. Functional Block Diagram of a B-VHF Receiver with Interference Suppression

Analogue RFI Cancelling

Since the signal power of a local DSB-AM interferer can be considerably high at the B-VHF receiver, it might cause signal clipping in the ADC. To avoid this, an analogue RFI canceller first has to suppress the RFI to the level of the desired signal. Two kinds of interferers can be suppressed in the analogue front-end, the own transmitted DSB-AM signal and the carrier signal of strong interferers. Since the own transmitted DSB-AM signal is known, the suppression of this signal at the B-VHF airplane receiver can be efficiently performed by simply subtracting it from the B-VHF receive signal. With this approach, a reduction of 30 to 40 dB is achievable.

The carrier power of a strong DSB-AM interferer can be estimated in the digital domain and

subtracted at the analogue side. Figure 14 shows this interference module. A DSB-AM signal waveform is

$$f(t) = A_c\left[1 + m \cdot s(t)\right]\cos\left(2\pi f_c t + \varphi\right), \quad (2)$$

where $s(t)$ is the modulating baseband signal, A_c and f_c are the amplitude and the carrier frequency of the radio frequency, and m is the modulation index. Thus, the total transmitted power P_T is

$$P_T = \frac{A_c}{2}\left(1 + \frac{m^2}{2} \cdot \left\langle s^2(t)\right\rangle\right) \quad (3)$$

for a Direct Circuit (DC) free signal and the additional condition that $\max\left(\left|m \cdot s(t)\right|\right) \le 1$.

Assuming $m = 1$ and a crest factor of 0 dB the maximum power in the DSB-AM sidebands is 50% of the carrier power. Therefore, the suppression of the carrier in a DSB-AM signal will reduce the power of at least 4.77 dB for a signal with a crest factor of 0 dB. A typical crest factor for a speech signal is around 12 dB, hence, the interference power reduction obtainable by only suppressing the carrier is usually around 17 dB.

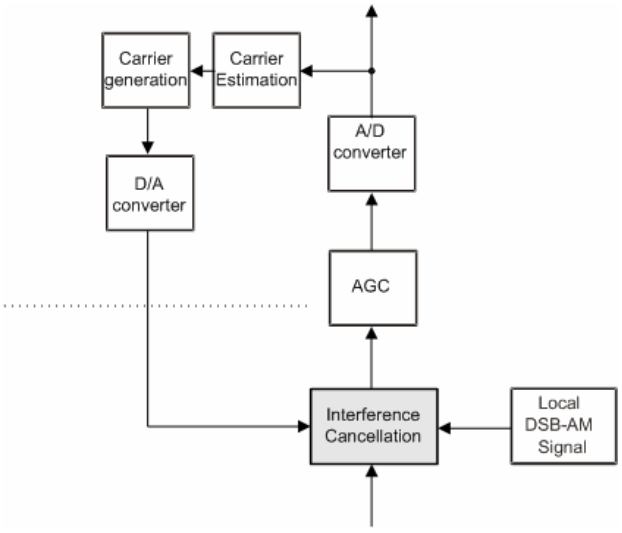

Figure 14. Functional Block Diagram of an Analogue DSB-AM Interference Cancellation Module

Digital RFI Cancelling – Time Domain Processing

Figure 13 presents a reference model for the B-VHF receiver. Notching the interferers can be applied not only in the analogue but also in the digital domain. Fixed digital band-stop filters are normally less attractive because they cause unaccepted high inter-symbol and inter-carrier interference levels. However, in the B-VHF system spectral areas are intentionally excluded in which strong interferers occur. In these areas a notch filter would be the right option, since phase distortion in the blocking band has no influence on the B-VHF signal.

RFI seriously degrades the performance of a B-VHF receiver as a result of the well-known leakage effect. Because of the relatively high sidelobe characteristic of the rectangular window, the effect of a narrowband interferer is not limited to a single tone but is spread over a large number of consecutive sub-channels. Therefore, a narrowband interferer disturbs the whole OFDM symbol. To reduce this spectral spill over, additional windowing can be applied at the receiver. In most cases the window resembles a RC shape as already described for windowing at the transmitter. Again, the drawback of windowing is that the system throughput is reduced as the OFDM symbols must be further prolonged in time.

Frequency Domain Interference Cancellation

As explained earlier, a narrowband RFI will not only affect the sub-carriers within its frequency range but also affects neighbouring sub-carriers due to the leakage effect. If the exact frequency location of the interferer is known, as well as its amplitude and phase, its disturbance on each sub-carrier can be calculated [11]. The presence and position of a narrowband interferer can be obtained by observing the noise on each of the sub-carriers. An unmodulated sub-carrier can be reserved in each RFI band to calculate the average amplitude and phase of the interferer. Several reserved sub-carriers per RFI band are required to cancel multiple interferers. To calculate the contribution on a given sub-carrier, the reserved sub-carrier is multiplied with a complex coefficient whose value can be derived from the characteristic filter associated with the receiver window. The result of this

multiplication is subtracted from the considered sub-carrier to cancel the effect of the narrowband interferer. The canceller is able to suppress several strong narrowband interferers simultaneously. In combination with windowing, it reduces interference by 30 to 40 dB [11].

Soft Erasure Technique

The frequency diversity available in B-VHF due to the CDMA or CDM component enables the application of a soft erasure technique. This technique evaluates each sub-carrier, where a chip of a data symbol is transmitted. In an overlay system each sub-carrier is affected by a complex channel coefficient and in addition by interference from the legacy VHF systems. In OFDM the problem of equalization is reduced to estimating the complex equalization value for each sub-carrier. The equalizer control unit should not only take into account the channel disturbance but also the current interference state information (IFSI). In [10], the equalisation value is weighted by an estimated interference value such, that the chips in corrupted sub-channels contribute less than chips in non-corrupted sub-channels. The results in [10] show that this "soft-erasing" technique performs very well, when the interference is modelled as a number of continuous sine waves. The sine wave interferers could disturb up to 50% of the sub-carriers resulting in a degradation of less than 4 dB. If the interferers are DSB-AM signals the degradation will be higher. Nevertheless, the technique can be used to weight the sub-carriers according the current IFSI.

IV. Performance Results

In this section, performance results that illustrate effectiveness of the described sidelobe suppression methods are given assuming a simple B-VHF overlay system. The considered system parameters are as follows. BPSK modulation is applied. The observed bandwidth consists of five 25 kHz channels enumerated with #1, #2, #3, #4, and #5. It is assumed that the channels #2 and #4 are available for transmission of the B-VHF signal, whereas the channels #1, #3, and #5 are occupied by 'strong' VHF interferers. The sub-carrier spacing is set to $\Delta f = 2.083$ kHz, hence, enabling 12 sub-carriers within a 25 kHz channel. The sidelobe suppression is performed applying windowing or windowing in combination with CCs. An RC window with $\alpha = 0.2$ is used. In the case CCs are applied, 4 sub-carriers are reserved as CCs within each 25 kHz channel – 2 on the left and 2 on the right side. As a result, in the case of CCs, 8 sub-carriers are available for data transmission within each 25 kHz channel, i.e., we have altogether 16 data sub-carriers in channels #2 and #4. The normalized PSD of the B-VHF signal caused by the transmission from channels #2 and #4 is illustrated in Figure 15 for the symbol vector $\mathbf{d} = (1,1,1,1,1,1,1,1)^T$. The benefits of the combination of RC windowing and CCs are clearly visible, since the sidelobes are significantly better

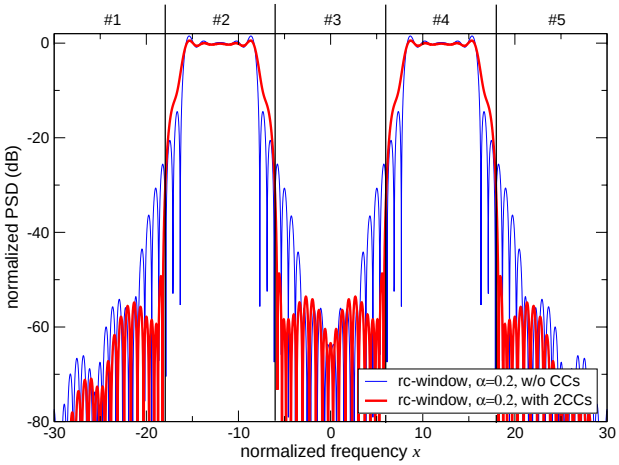

Figure 15. Spectrum of B-VHF Signal Assuming B-VHF Transmission in 25 kHz Channels #2 and #4; $\mathbf{d} = (1,1,1,1,1,1,1,1)^T$

The mean PSD over all possible data symbol sequences considered separately in the channels #1, #3, and #5 is illustrated in Figure 16. Simulation results are given for the cases when only RC windowing as well as when RC windowing in combination with CCs is applied. The sidelobe power averaged over all sequences, assuming that only RC windowing is applied, is -42.0 and -37.6 dB in channels #1 & #5 and in channel #3, respectively. The combination of RC windowing and CCs leads to substantial sidelobe suppression. In such a case the sidelobe power averaged over all sequences is -54.4 dB in channel #1 & #5 and -50.4 dB in channel #3. It is noticeable that, among all the channels in which the sidelobe power is observed, the highest sidelobe power is in channel #3, since in

this particular channel the sidelobes originating from the channels #2 and #4 constructively add.

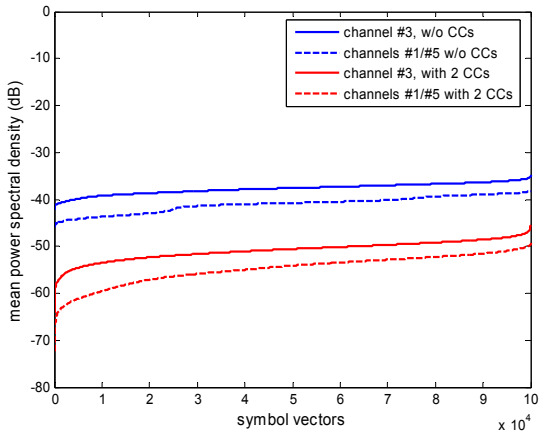

Figure 16. Mean PSD of Sidelobes of All Possible BPSK Symbol vectors with and without CCs; RC Windowing with $\alpha = 0.2$

V. Conclusions

In this paper, the basic physical layer aspects of an overlay system based on MC technology in the VHF band are described. Based on that, the main MC system design challenges specific for an overlay concept are recognized. In addition, solutions to the most severe of these challenges are provided. Special emphasis is put on the successful co-existence of the VHF legacy systems and the B-VHF system. Numerical results show that by applying the appropriate countermeasures the interference from B-VHF to the VHF legacy systems can be successfully suppressed.

References

[1] http://www.b-vhf.org

[2] M. Schnell, E. Haas, C. Rihacek, and M. Sajatovic, "B-VHF – An Overlay System Concept for Future ATC Communications in the VHF Band," Proc. 23rd Digital Avionics Systems Conf. (DASC 2004), Salt Lake City, USA, Oct. 2005.

[3] K. Fazel and S. Kaiser, Multi-Carrier and Spread Spectrum Systems, West Sussex: John Wiley & Sons Ltd, 2003.

[4] R. van Nee and R. Prasad, OFDM for Wireless Multimedia Communications, Boston, London: Artech House, 2000.

[5] S. Brandes, I. Cosovic, and M. Schnell, "Reduction of Out-of-Band Radiation in OFDM Based Overlay Systems," submitted to IEEE Symposium on Dynamic Spectrum Access Networks (DySPAN 2005), Baltimore, USA, Nov. 2005.

[6] J. Bingham, "RFI Suppression in Multicarrier Transmission Systems," Proc. IEEE Global Telecommun. Conf., (GLOBECOM'96), London, UK, Nov. 1996.

[7] S. Brandes, I. Cosovic, and M. Schnell, "Sidelobe Suppression in OFDM Systems by Insertion of Cancellation Carriers," Proc. IEEE Vehicular Technology Conf. (VTC´05 Fall), Dallas, USA, Sep. 2005.

[8] I. Cosovic, S. Brandes, and M. Schnell, "A Technique for Sidelobe Suppression in OFDM Systems," Proc. IEEE Global Telecommun. Conf. (GLOBECOM'05), St. Louis, USA, Dec. 2005.

[9] L. de Clercq, M. Peeters, S. Schelstraete, and T. Pollet, "Mitigation of Radio Interference in xDSL Transmission," IEEE Communications Magazine, pp. 168–173, March 2004.

[10] K. Fazel, "Narrow-Band Interference Rejection in Orthogonal Multi-Carrier Spread-Spectrum Communications," Proc. IEEE ICUPC'94, 1994.

[11] F. Sjöberg, R. Nilsson, N. Grip, P.O. Börjesson, S.K. Wilson, and P. Ödling, "Digital RFI Suppression in DMT-based VDSL Systems," Proc. Int. Conf. on Telecommun. (ICT'98), Chalkidiki, Greece, Jun. 1998.

Email Addresses

I. Cosovic, Ivan.Cosovic@dlr.de

S. Brandes, Sinja.Brandes@dlr.de

M. Schnell, Michael.Schnell@dlr.de

B. Haindl, Bernhard.Haindl@frequentis.com